PAPER • OPEN ACCESS

Effect of hydrodynamic load modelling on the response of floating wind turbines and its mooring system in small water depths

To cite this article: Kun Xu *et al* 2018 *J. Phys.: Conf. Ser.* **1104** 012006

View the article online for updates and enhancements.

IOP ebooks™

Bringing you innovative digital publishing with leading voices to create your essential collection of books in STEM research.

Start exploring the collection - download the first chapter of every title for free.

Effect of hydrodynamic load modelling on the response of floating wind turbines and its mooring system in small water depths

Kun Xu[1], Zhen Gao[1,2], Torgeir Moan[1,2]

[1] Department of Marine Technology, Norwegian University of Science and Technology (NTNU), Trondheim, NO-7491, Norway
[2] Centre for Autonomous Marine Operations and Systems (AMOS), NTNU, Trondheim, NO-7491, Norway

E-mail: `kun.xu@ntnu.no`

Abstract. A large number of offshore wind turbines have been installed recently, mostly in water depth up to 30 m based on monopile foundations. It is expected that floating wind turbine becomes more competitive than bottom fixed wind turbine when the water depth exceeds 50 m. In this paper, the focus is on the environmental loads and responses of mooring systems for a semi-submersible in water depths from 50 m to 200 m. Mooring design for moderate water depths is relatively easy to achieve, but it is challenging for shallow water. The effect of environmental load modelling should be studied based on designing a reasonable mooring system. With a mooring system design for 200 m water depth as a reference, two mooring system design concepts in 100 m and 50 m water depth have been proposed for a 5-MW-CSC semi-submersible floating wind turbine. Preliminary design has been carried out to determine mooring line properties, mooring system configurations and document the static performances. A fully coupled time domain dynamic analysis for extreme environmental conditions was performed using Simo-Riflex-AeroDyn. Four different load models were applied in order to check the influence of different load components including the effect of wind, current and second order wave forces by means of Newman's approximation and a full QTF method.

1. Introduction

In the last decades, more and more offshore wind energy projects have emerged with the purpose to accommodate more wind power with better quality, avoid noise effect and visual disturbance to citizens and achieve less obstacle to transport. Through the experiences gained in the offshore oil and gas industry, the long-term survivability of offshore support structures has been successfully demonstrated in the wind energy industry. There is still a huge potential for cost reduction and technological innovation. All ongoing commercial scale offshore wind projects utilise seabed mounted substructure concepts. However in many countries there are only a limited number of suitable sites in sufficiently shallow water to allow economically viable fixed substructures to be deployed. When the water depth exceeds 50 m, floating support structures are expected to be competitive in terms of lifecycle cost. However, floating wind turbines are still at an early stage of development and it is of vital importance to identify the marginal depth to make floating wind turbines competitive.

EERA DeepWind'2018, 15th Deep Sea Offshore Wind R&D Conference

IOP Publishing

IOP Conf. Series: Journal of Physics: Conf. Series **1104** (2018) 012006

doi:10.1088/1742-6596/1104/1/012006

A semi-submersible platform achieves stability by water plane stiffness and ballast in the columns or pontoons to some extent. The characteristic of small draft of semi-submersible allows it to be deployed in shallow waters. There has been several successful semi-submersible floating wind turbine projects all over the world, such as WindFloat [1], OO Star Wind Floater [2], 5-MW-CSC semi-submersible floater [3], Fukushima FORWARD demonstration project [4].
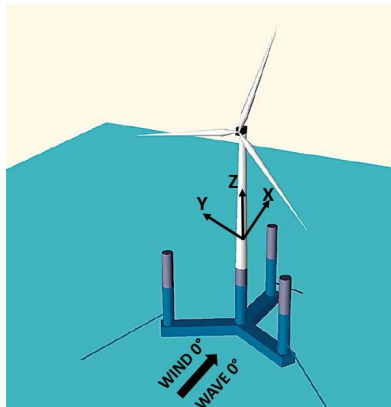
Hull steel mass	1686	t
COG	(0, 0, -24.53)	m
COB	(0, 0, -22.42)	m
Draft	30	m
Pontoon length	41	m
Pontoon height	6.0	m
Column length	24	m
Column diameter	6.5	m
Floater draft	30	m

Figure 1. Overall layout[3] and main properties[5] of 5MW-CSC floater

The 5-MW-CSC semi-submersible floating wind turbine studied in this paper includes a wind turbine, a tower, a semi submersible hull and three catenary mooring lines, as shown in Figure 1. The origin of the coordinate system is placed at the still water level with wave and wind direction as shown. The braceless semi hull consists of three pontoons, three side columns and one central column supporting the tower and the wind turbine [6]. The wind turbine in the study is the NREL 5 MW reference wind turbine [7] mounted on the OC3 Hywind wind tower [8] which starts from 10 meters above the waterline.

The purpose of this paper is to study the effect of different environmental loads on floating wind turbine motion and mooring system. Three water depths were considered in order to address the challenge to design mooring system at small water depth and to check the variation of responses while same environmental conditions are used. Based on preliminary design, three mooring systems were proposed to carry out the analysis. No detailed design and design optimization were performed since they served the purpose quite well.

2. Theory

2.1. Wave loads

Wave loads acting on the floating structure can be estimated based on potential flow theory or Morison formula using wave kinematics. The Morison formulation is mainly applied for slender structures with small dimensions compared to the wave length. As for large volume structures, diffraction and radiation forces are important. Therefore, in this paper, the potential flow theory is used to calculate the hydrodynamic loads acting on the floater while Morison formulation is applied to calculate wave forces on the mooring line.

Potential flow theory considers the solutions of a linearized boundary value problem for inviscid, incompressible flow. For the first order linear wave solutions, the loads and motions have zero mean value and oscillate with the frequency of the incident waves. When it comes to loads and motions of a semi-submersible platform, the slow drift motions caused by slowly-varying (slow drift) loads connected with second order difference frequency effect and mean drift effect become important [9]. The contribution from second order potential is the most difficult part to compute which is required to satisfy the second order free surface boundary condition

and an additional free surface mesh is needed to solve the problem numerically. The resulting force can be written as:

$$F_j^{(2)} = \Re \sum_m \sum_n \xi_m \xi_n T_{mn}^j(\omega_m, \omega_n) e^{-i(\omega_m - \omega_n)t + (\epsilon_m - \epsilon_n)} \tag{1}$$

The function $T_{mn}^j(\omega_m, \omega_n)$ represents the complex difference frequency second order transfer function, known as the quadratic transfer function (QTF).

Since a catenary mooring system is considered, only difference frequency wave loads are used in the analysis regarding induced resonant motions in surge, pitch and heave. Due to the difficulty in calculating QTFs, some approximations have been proposed, mainly to avoid computing the second order velocity potential $\phi^{(2)}$. One of the most widely used methods is Newman's approximation, which could be used to derive the QTF matrix based on the mean drift forces which is depended only on the first order solutions.

Newman's approximation becomes inaccurate when the frequency considered is close to resonance condition with small damping and the accuracy also decreases for motions with low natural period, e.g. for heave, pitch and roll motion. Therefore in this paper:

- Newman's approximation will be only considered in horizontal motion, i.e. surge, sway and yaw motion to account for second order difference-frequency wave loads.
- Full QTF method will include the contributions from all six degree of freedoms.

2.2. Wind loads

A structure under the influence of wind will experience static and dynamic wind forces. The wind loads acting on the nacelle and tower are primarily drag forces. However, the loads acting on the blades include both lift and drag forces, which can be calculated with blade element momentum (*BEM*) and generalized dynamic wake (*GDW*) [10]. In this paper, *BEM* theory is used when the mean wind speed is below 8 *m/s*, otherwise, *GDW* theory is chosen. The wind field is generated by *TurbSim* [11] based on the Kaimal spectral model. The turbulence intensity is defined in *IEC 61400* standard [12]. *Class C* is selected in current study for offshore condition. Meanwhile, *Extreme Wind Model* is used for extreme condition related to parked model.

2.3. Current loads

The slow-drift motion of moored floating structure is greatly influenced by second order difference-frequency wave loads, wind loads and current loads. The wave drift forces will increase when current load is involved [13]. Viscous drift forces due to wave-current interaction effects is important to consider especially in extreme sea states [14]. Therefore, according to [15], the effect of current loads on mooring lines should be taken into account when relevant. Current velocity vector varies with water depth, while the profile is stretched or compressed due to surface waves. Generally, the current velocity can be considered as a steady flow field where the velocity vector is only a function of the water depth [16]. The current profile considered in this paper is wind-generated current expressed as a linear profile from still water level to a certain depth below which the current is assumed to vanish.

3. Preliminary design of mooring system

The purpose of this paper is to compare the effect of different hydrodynamic modelling on the response of mooring system and floater motion, therefore reasonable mooring systems are needed at different water depths. According to [15], the mooring system must fulfil three safety criteria: ULS, FLS and ALS. Due to the configuration, it can be quite challenging to ensure system integrity in ALS condition when losing one or more mooring lines. In this paper, ULS condition

was the main criteria considered to propose mooring system design concepts. The main criteria in the preliminary design for mooring system to follow, includes:

(i) Stiffness criterion: The horizontal stiffness of the mooring system should be sufficient to keep the platform within a specific range and compliance to reduce the tension in first order waves. Moreover, there should not be vertical force acting on the anchor in order to prevent lifting up the anchor.

(ii) Resistance criterion: The mooring lines should be strong enough to ensure normal operation, in other words, the maximum line tension should not exceed the capacity of the mooring line.

(iii) Design loads are carried out based on partial safety factors for the tension (load effect) due to mean and dynamic tension depending on the consequences of failure.

(iv) In the design phase, power cable design is carried out when the mooring system configuration and the maximum offset are determined. Power cable is then designed to accommodate the possible maximum offset. This design philosophy determines that the floater motion should be limited to a reasonable range especially in horizontal plane in order to protect the power cable from taking large loads and bending moments.

Essentially, the challenge in mooring line design is to balance stiffness and strength. In this connection, the fact that the tension increases in a nonlinear fashion which will cause large tension due to geometrical effect for catenary mooring lines is an important issue to consider.

3.1. Reference mooring system - 200 m water depth
The initial 5-MW-CSC floating wind turbine is designed for 200 m water depth, which has been utilized as a reference model in order to carry out the study for 100 m and 50 m. The mooring system consists of three catenary mooring lines which are made of spiral rope and positioned with 120 degrees angle between the mooring lines. Each mooring line is attached at the outer columns of the semi at a water depth of 18 meter, where the fairlead is located. The configuration of upper part is close to a straight line because of the clump weight, while the lower part has a catenary shape. The anchor used here is a conventional fluke anchor which is mounted into the seabed.

Table 1. Mooring line properties for 200 m, 100 m and 50 m

Water Depth (m)	200	100	50
Mooring line type	Spiral rope	Spiral rope	Chain R4-RQ4
Nominal diameter (m)	0.1365	0.1365	0.18
Nominal cross-section area (m^2)	0.01465	0.01465	0.0509
Gyration radius (m)	0.03415	0.03415	0.0636
Mass/length in air (kg/m)	115.02	115.02	648
Axial stiffness per unit length (KN/mm)	3.08E6	3.08E6	2.92E9
Transversal drag coefficient	1.2	1.2	2.4
Longitudinal drag coefficient	0.02	0.02	1.15
Transversal added-mass coefficient	0	0	1
Longitudinal added-mass coefficient	1	1	2
Catalogue breaking load (KN)	16769	16769	26278

3.2. Mooring system for 100 m and 50 m water depths
Based on a satisfactory mooring system design for 200 m water depth, the evaluation criteria of preliminary design for 100 m and 50 m is to achieve the similar stiffness, catenary shape and

pretension as in 200 m. Since the same floating wind turbine is utilized for 100 m and 50 m, the general mooring line configurations are kept the same as in the reference model. A longer part lying on the seabed for shallower water depth is under expectation in order to prevent mooring line from being totally lifted up and prevent vertical force acting on the anchor. For catenary mooring system, the suspended length of mooring line decreases with water depth, which will further influence the pretension which is mainly determined by self-weight of suspended mooring line and clump weight. In order to compensate for this feature, heavier mooring line material - studless chain $R4 - RQ4$ is selected for 50 m and wire rope is selected for 100 m. Generally, the weight of chain is about five times of the wire rope, which could be beneficial to achieve the desired pretension in 50 m water depth. It is recommended to use spiral strand when the required service life of mooring system is more than 20 years [15]. In addition, corresponding clump weights in 100 m and 50 m have been enlarged as well. Furthermore, in order to improve the fatigue performance, a HDPE plastic sheathing is used for spiral rope and no stud is utilized to connect chain links.

Table 2. Mooring system configuration for 200 m, 100 m and 50 m

		200	100	50
Water Depth (m)		200	100	50
Mooring line number		3	3	3
Angle between adjacent lines (deg)		120	120	120
Depth from fairlead to seabed (m)		182	82	32
Radius from fairlead to platform center (m)		44.25	44.25	44.25
Radius from anchor to platform center (m)		1184.5	917	720
Initial Configuration	Offset at fairlead (m)	0	0	0
	Angle at fairlead(deg)	59.9	56.5	40.9
	Total length (m)	1173	891.6	686.6
	Suspended length (m)	711.6	336.8	80.6
	Touchdown length (m)	461.4	554.8	606
Extreme Configuration	Offset at fairlead (m)	17	18	20
	Angle at fairlead(deg)	73.4	80.6	84.1
	Total length (m)	1173	891.6	686.6
	Suspended length (m)	1148	881.5	675.6
	Touchdown length (m)	25	10.1	11

In order to check the static performance of the proposed concepts for 100 m and 50 m water depths, a comparative study is carried out with respect to the performance of 200 m design. According to the result shows in Figure 2, the tension increases in a nonlinear behaviour which is applicable for all three water depth while it becomes more significant when water depth decreases. The behaviour occurs at smaller offset for 50 m water depth.

4. Hydrodynamic load modelling and analysis
HydroD (Wadam) based on potential wave theory is used to carry out hydrodynamic analysis of the semi-submersible platform. Additionally, second order free surface boundary condition has to be fulfilled in order to calculate full QTF, which requires an additional free surface mesh to solve the problem numerically. The hydrodynamic model is provided in Figure 3.

4.1. Free decay test
Free decay tests are carried out to estimate the natural periods of floater motions and damping. The decay tests for 5-MW-CSC floater are performed at the undisturbed position in six degrees of freedom and three water depths. The damping is very important when the load acting excites
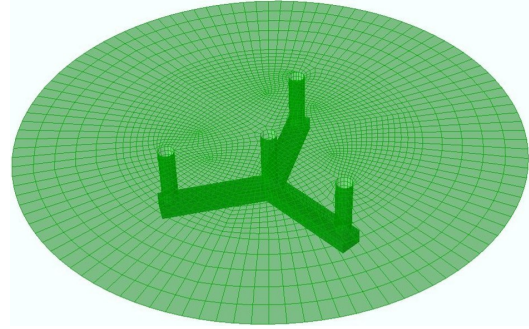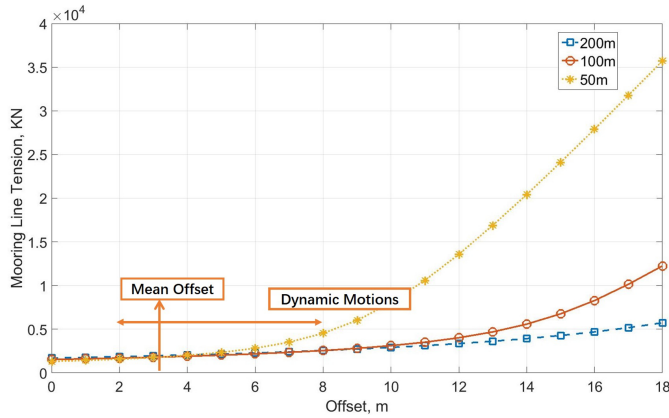
Figure 2. Mooring line tension with offsets for water depth of 200 m, 100 m and 50 m.

Figure 3. Hydrodynamic model in HydroD.

the resonant motion of the structure. The magnitude of the damping determines the amplitude of the resonance. The damping included in this paper includes: potential wave excitation damping, viscous damping effect acting on the floater and viscous damping on the mooring line by means of the drag force in Morison's formula.

4.2. Load cases
Based on the data from [17], Norway site 5 has been selected as a representative site for a floating wind turbine. The environmental condition corresponding to 50-year wind, wave and 10-year current conditions are listed. Two typical extreme environmental conditions corresponding to 50 years condition are provided for Norway site 5 suggested by [17] with one refers to the condition with maximum mean wind speed and one condition with maximum significant wave height as shown in Table 3.

Table 3. Extreme load cases for 50-year wind, wave[17] and 10-year current[15]

Condition	U_w	H_s	T_p	U_c	Turbine status
	[m/s]	[m]	[s]	[m/s]	
ULS-1	41.86	13.4	13.1	1.05	Parked
ULS-2	38.87	15.6	14.5	1.05	Parked

As for the current profile, a surface current speed (U_c) with a 10-year return period is recommended to use according to[15]. Currently there is no available statistical data of current speed of Norway site 5. However, it can be estimated based on the mean wind speed:

$$U_w = 0.015 \cdot U_c \tag{2}$$

Besides, Norway site 5 is located quite close to location North sea (Troll) whose recommended current speed with 10-year return period is *1.5 m/s* according to [15]. Therefore, the final current speed used in this paper is taken as the average of the estimated value and the value for location Troll platform. The variation is considered as a linear profile from *z= -50 m* to still water level and it is assumed to vanish at 50 m below the still water level. The same current profile is used for all three water depths.

$$U_c(z) = 1.05 \cdot \left(\frac{50 + z}{50} \right) \quad for \quad -50 \le z \le 0 \tag{3}$$

In order to check the influence of the effect of different methods to include second order wave force and the effect from wind force, four different load models have been included in this paper:

Table 4. Hydrodynamic Load models

No	Wave		Wind	Current
	First-order	Second-order		
1	Included	Not included	Not included	Included
2	Included	Newman's approximation (3 DOF)	Not included	Included
3	Included	Full QTF (6 DOF)	Not included	Included
4	Included	Full QTF (6 DOF)	Included	Included

The Newman's approximation is good if the frequency difference is small, which is usually the case for horizontal motions for offshore structure especially in deep water. Newman's approximation is uncertain when it comes to shallow water. Comparing results from models 1, 2 and 3, the accuracy of Newman's approximation for second order wave forces can be judged. By comparing results from model 3 and 4, the influence from wind force could be figured out. Meanwhile, drag force on mooring line is included for all the models as the third contribution to second order response. Current is considered for all the models as well. In addition, four wave directions have been selected in order to check the influence of wave-wind misalignment: $0°$, $45°$, $60°$ and $90°$.

4.3. Fully coupled dynamic model
Taking the current study objective - offshore floating wind turbine into account, factors such as turbulent wind field, nonlinear wave loading, nonlinear structural behaviour and servo control make it necessary to carry out fully coupled aero-hydro-servo-elastic analysis to capture the nonlinear responses. In this paper, the fully coupled dynamic simulation is run for 4000 s with time step of 0.01 s which corresponds to a one-hour dynamic analysis while the first 400 s is eliminated because of start-up transient effects. For each load case and each wave direction, 5 identical and independent one-hour simulations with different seed numbers for the turbulent winds and irregular waves were carried out to reduce the statistical uncertainty. The final statistics e.g. maximum, mean and standard deviation were calculated by averaging the results from the five samples.

5. Results and discussions
5.1. Spectral analysis
The floater motion response spectrum with 0 deg incoming wave direction in ULS-1 condition is discussed as an example. Three water depths and four load models are listed together for comparison. Generally speaking, the second-order forces are small compared to the first-order forces. However, when the difference-frequency forces coincide with the eigenfrequencies of the structure, some resonant motions will occur. The wind force is included in the fourth model, however the effect from mean wind force is not significant because the turbine is in a parked condition. There is great similarity regarding the spectrum in ULS-1 condition and ULS-2 condition, therefore only results from ULS-1 condition is listed.

Floater motion

- For **surge** motion, the wave frequency response is dominated by the frequency range of 0.3 to 0.7 rad/s and they are larger in the 50 m case due to the intermediate wave depth effect as compared to the 100 m and 200 m cases. Similarly, the surge resonant motion is also larger. In addition, there is a low frequency response around 0.1 rad/s, which is due
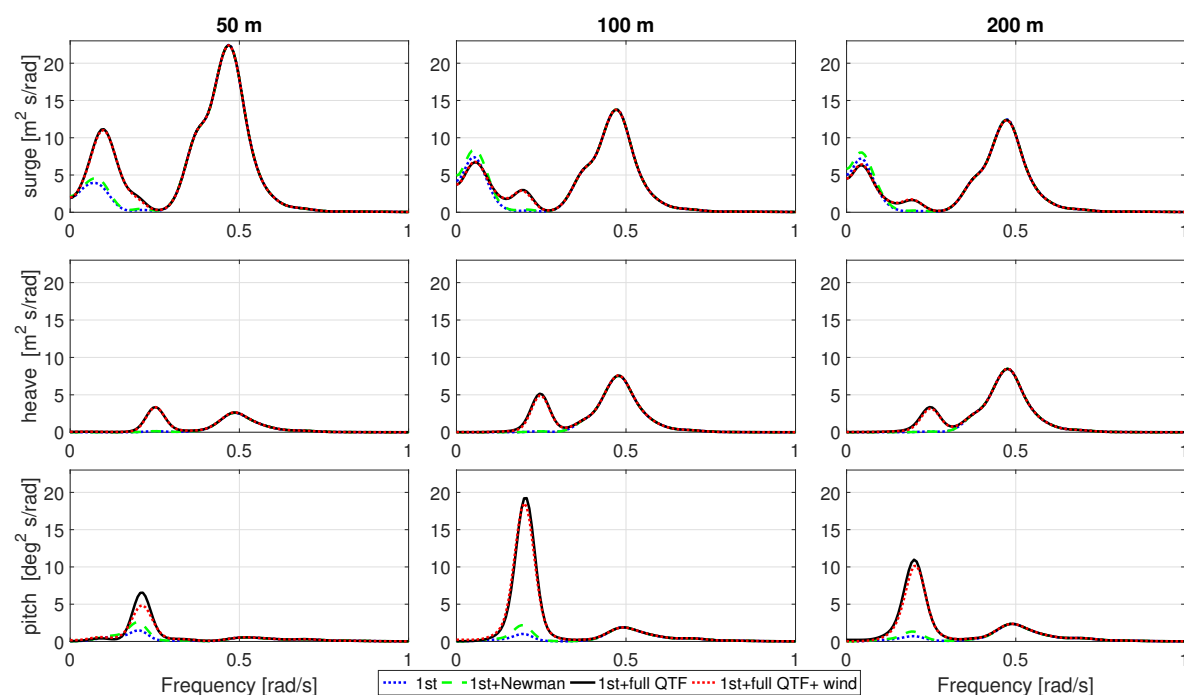
Figure 4. Floater motion spectrum in ULS-1 condition

to surge resonance. Moreover, the coupling between surge and pitch also contribute to the total motion response. A small peak is observed at about 0.2 rad/s which coincides with pitch resonant frequency. The coupling effect is not significant for the 50 m case.

- For **heave** motion, wave frequency response is still dominating in the same range. The heave resonant motion occurs at 0.25 rad/s for all three water depths. Second-order difference frequency response in heave motion is more significant than surge motion. However, the amplitude is still smaller than the wave frequency response.

- For **pitch** motion, the pitch resonant contribution is in leading position at 0.2 rad/s larger than wave frequency contribution, which makes it different from other responses. This is because pitch motion is quite sensitive to difference-frequency force and wind-induced force.

When comparing Newman's approximation and a full QTF with respect to represent second-order difference-frequency response, full QTF is supposed to provide the most accurate result for all six degrees of freedom while Newman's approximation is not good for surge resonant motion in small water depth. Besides, Newman's approximation does not apply to the resonant vertical motion, e.g. heave and pitch motion. Therefore, Newman's approximation of the low-frequency motion is clearly seen in Figure 4 to underestimate especially heave and pitch motion. A full QTF method is recommended to model difference-frequency force in order to better capture the low-frequency motion.

However, the wave-frequency range response does not seem to be influenced as expected. Therefore, the curves representing four different models coincide with each other at wave frequency in the spectrum. Since the wind turbine is in a parked condition during the ultimate limit state test, the influence from wind force is not prominent. Under such condition, the mean pitch motion is quite small. During operational condition where rotor rotates, large pitch motion due to thrust force can be expected and so is the response due to wind force.
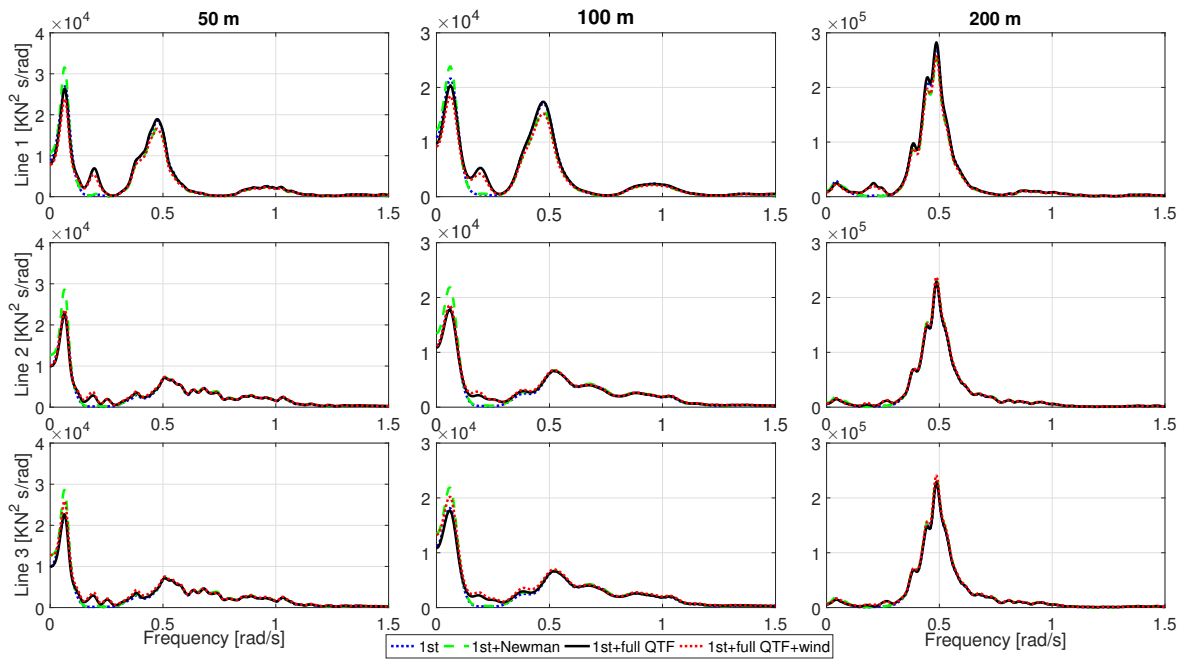
Figure 5. Mooring line tension spectrum for the ULS-1 condition

Mooring line tension

The spectrum for three mooring lines tension in head sea for the ULS-1 condition are shown in figure 5. The scales of the figure are chosen differently for different water depth for better indication due to the big difference of the magnitudes. The most significant contribution to the mooring line tension comes from wave frequency ranging from 0.3 to 0.7 rad/s, which applies to all three water depths. The difference among the four different load models are not significant in 200 m, which indicates that wave-frequency response is dominating while low-frequency response does not contribute much to the total response. However, the contribution from low-frequency response increases with decreasing water depth. The peaks between 0 to 0.3 rad/s in 100 m and 50 m stands for the contribution from difference frequency wave loads and aerodynamic loads including contribution from surge resonance around 0.1 rad/s and pitch resonance around 0.2 rad/s. Second-order surge resonant motions increase when the water depth decreases and so does the dynamic mooring line tension. Take the spectrum in 50 m as an example, the contribution from difference-frequency response does contribute a lot to the total response and it becomes more and more significant with decreasing water depth. Newman's approximation method underestimate the difference-frequency response compared with full QTF method.

5.2. Platform motion

In order to focus on the most critical motion response, only surge, heave and pitch motion were selected. The misaligned wave-wind condition was studied for all four cases, however only the result from 0° and 60° are listed because of the similarity. The effect of second order difference frequency force and wave-wind misalignment were the main focusing points as well as the water depths. Figure 6 and 7 shows the platform motion responses in three water depths with two wave incoming directions. The circle marker indicates the mean response with error bar standing for the standard deviation. The diamond marker represents the maximum response. Results for four different models at same water depth and load case are assembled together for better comparison. The total motion response is composed of a mean static response due to
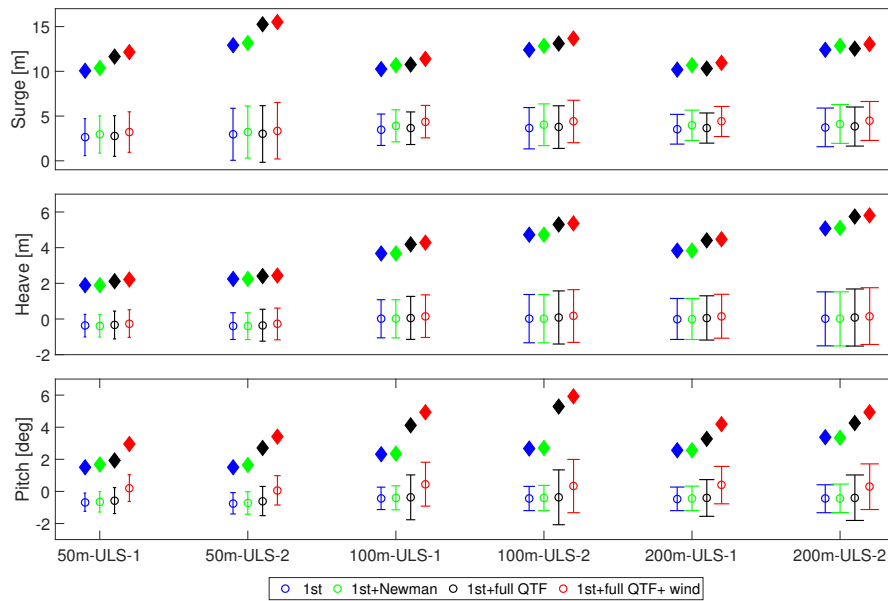
EERA DeepWind'2018, 15th Deep Sea Offshore Wind R&D Conference

IOP Publishing

IOP Conf. Series: Journal of Physics: Conf. Series **1104** (2018) 012006

doi:10.1088/1742-6596/1104/1/012006

Figure 6. Motion response for three water depths with 0° wave and wind incoming direction

mean wave and wind force together with a dynamic response due to wave frequency and low frequency response. Generally speaking, the motion responses are larger in ULS-2 condition where the wave condition is more severe, which demonstrates that floater motion response is more sensitive to wave load rather than wind load. When comparing the three water depths, the amplitude is relatively larger in 50 m than 100 m and 200 m.
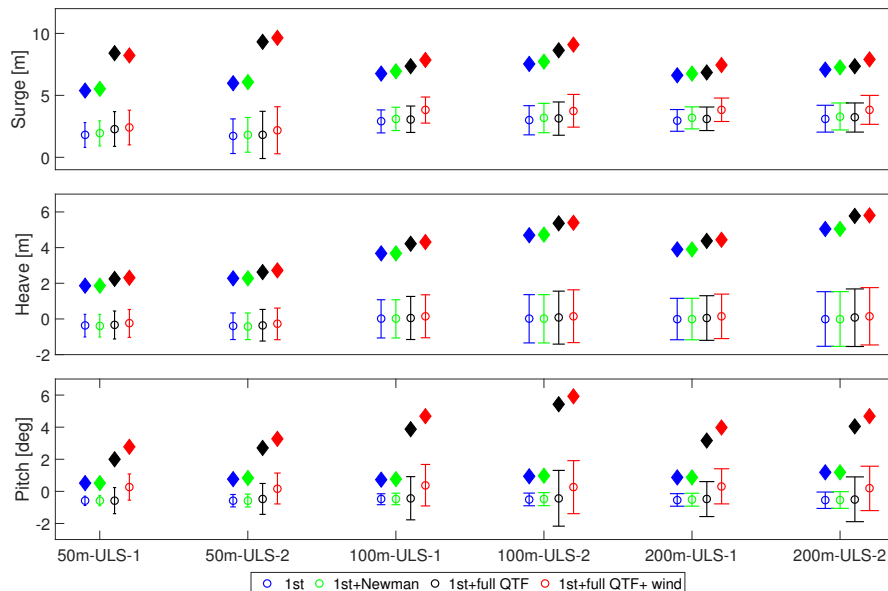

Figure 7. Motion response for three water depths with 60° wave direction and 0° wind direction

The mean values of the platform motions are mainly wind induced and the rotor is feathered in the ultimate limit case, therefore, the mean motion is not extremely large for all the cases.

However, when comparing the third and forth model, the influence from wind force did show up with slightly larger response when including wind force. The motion response is smaller when wave comes from 60° as shown in figure 7, because the load direction does not coincide with the motion direction. However, large mooring line tension is discovered because the wave load acts directly in-line with mooring system configuration. In general, the platform motion responses are larger when considering second order difference-frequency force using full QTF method. In other word, only including first order wave force or including difference-frequency force using Newman's approximation will underestimate the motion response.

5.3. Mooring line tension
Figure 8 and 9 shows the mean, maximum and standard deviation of tension in all three mooring lines in two extreme load cases. For most cases, the dynamic tension takes smaller part of the total force compared with mean tension part, which means that the mean static force due to wave and wind is dominating and the dynamic behaviour in wave frequency and low frequency are not strong. Therefore, the difference in the mean with four different load models is relatively small, which because pretension of the mooring line is dominating.
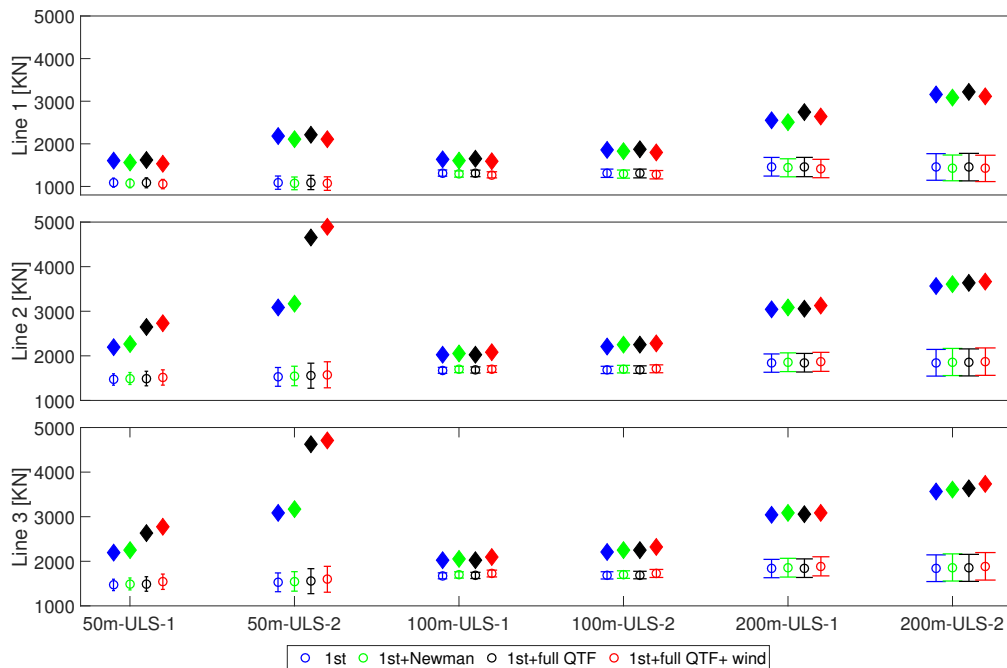

Figure 8. Mooring line tension for three water depths with wave incoming direction of 0°

However the second order difference-frequency wave force could lead to large response at resonance where damping will be important. Therefore, second order wave force did increase the maximum values and standard deviations. The maximum tension in 50 m case is much larger than the other two water depths which is due to the nonlinear tension increment when large offset was excited.

In ULS-2 condition where the significant wave height is larger, mooring line tension responses are relatively larger than those in ULS-1 condition for all the cases. Notably, the mooring line tension in 50 m increases significantly in ULS-2 condition. This is because the environmental condition, and especially the wave condition, has become severe enough to cause mooring line tension increase nonlinearly. Once the tension starts to increase nonlinearly, it will as expected be

more notable in shallow water. The mooring system in 100 m shows great performance without extreme tension increment, which indicates that the nonlinear behaviour is not significant in 100 m water depth. By comparing the mooring line tension response with different wave incoming direction, it is seen that the maximum mooring line tension occurs in the case when the wave loads are acting directly towards the mooring line, i.e. for mooring line 3 with 60° wave incoming direction for both conditions.
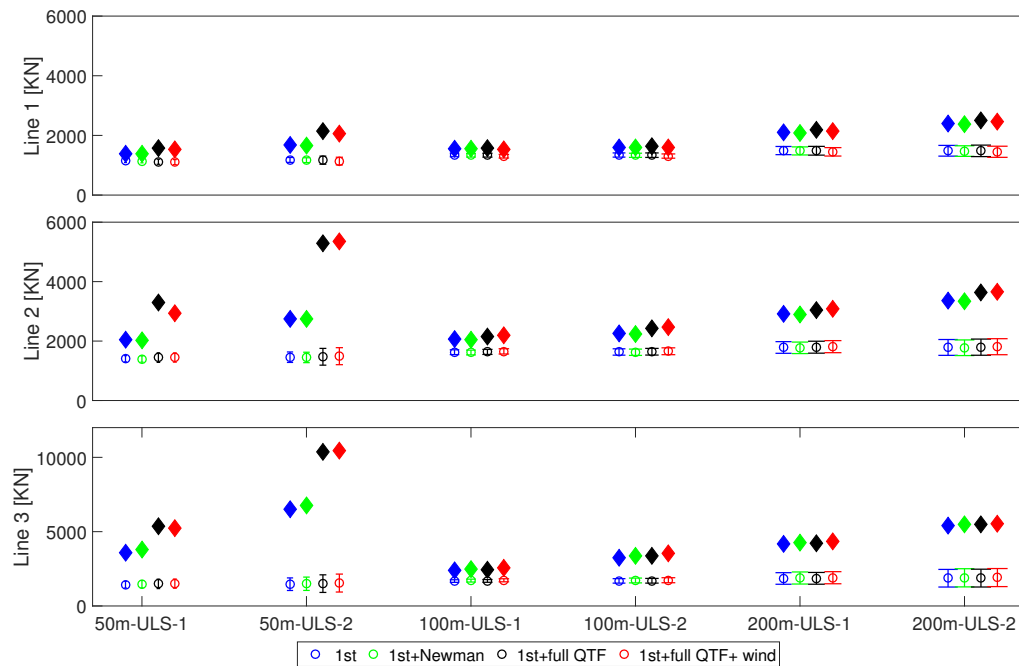

Figure 9. Mooring line tension for three water depths with wave incoming direction of 60°

It is notable that there is significant difference of maximum tension in different water depths even though the mean value and standard deviation seem quite close. When the mooring line tension follows a Gaussian process, the kurtosis of the response should be around 3 [18]. Moreover, the extreme tension can be expressed as:

$$M = \mu + k.\sigma \tag{4}$$

where M is the maximum value, μ is the mean value, σ is the standard deviation and k is coefficient with value of 4 for Gaussian process [20].

Table 5. Coefficient k and Kurtosis

	ULS-1-0			ULS-2-60		
	Moor1		Surge	Moor3		Surge
	k	Kurt	Kurt	k	Kurt	Kurt
50 m	4.3	3.4	3.5	14.7	49.0	3.7
100 m	4.4	3.5	3.2	10.8	19	3.2
200 m	5.7	5.4	3.1	6.0	6.1	2.9

The non-Gaussian nature of mooring line tension is greatly influenced by the nonlinearity of the mooring system which increases in shallow water as shown in Figure 2. Wave parameters e.g.

EERA DeepWind'2018, 15th Deep Sea Offshore Wind R&D Conference

IOP Publishing

IOP Conf. Series: Journal of Physics: Conf. Series **1104** (2018) 012006

doi:10.1088/1742-6596/1104/1/012006

significant wave height and wave peak period in the meanwhile also affect the Gaussian nature of the mooring line tension [21]. Larger kurtosis coefficient is expected in severe sea states. The k values in Equation 4 estimated for mooring line 1 tension in ULS-1 condition with $0°$ incoming wave direction and mooring line 3 tension in ULS-2 condition with $60°$ incoming wave direction are shown in Table 5. The kurtosis for surge motion in both cases are listed as well. The load model used here includes current load, wind load and second order wave load based on full QTF method.

For the surge motion, the kurtosis are close to 3 for all cases, which indicates that the motion is close to Gaussian process. As for the mooring line tension, the kurtosis for 50 m and 100 m water depth is close to 3 and k value close to 4 while both kurtosis and k value are slightly larger in 200 m water depth. This indicates that when the environmental condition is not extremely severe, tension for the least loaded mooring line almost follows a Gaussian distribution. Meanwhile, as the most loaded mooring line 3 in more severe sea state ULS-2 condition, there is significant increase in both the kurtosis and k value and they increase faster with decreasing water depth which displays the high non-Gaussian character.

Larger kurtosis indicates that higher extreme values exist in the upper tails of the probability density distribution [19]. In high sea states, non-Gaussian behaviour is expected in principle in floater motions and especially mooring line tension. The property will increase when the current is included [22].

6. Conclusion

During the mooring system design phase, two factors that can influence mooring line tension significantly were mainly considered: geometrical effect and increased stiffness for large offsets. In order to achieve similar performance, heavier mooring line was chosen for the shallow water depth with longer mooring line placing on the seabed.

As for the dynamic analysis, the mean response of the platform motion and mooring line tension which is due to mean wave and wind force are not affected by the difference-frequency effect. As water depth decreases, the contribution from difference frequency becomes increasingly more significant. Therefore in order to capture the low-frequency response accurately, a full QTF method is recommended while Newman's approximation will underestimate the response.

In the extreme condition, the maximum mooring line tension occurs in the case when the wave acting aligned with the mooring line configuration direction while the direction of wind and current are considered fixed. Mooring line tension and floater motions are relatively larger in the condition where wave is more severe, which indicates that they are more sensitive to wave loads than wind loads.

The highly non-Gaussian property of responses in high sea states indicates possible extreme mooring line tension and floater motion, which makes it quite challenging to design mooring system for extreme environmental conditions especially in shallow water.

References

[1] Roddier D, Peiffer A, Aubault A and Weinstein J. 2011 *Proc. of the ASME 2011 30th Int. Conf. on Ocean, Offshore and Arctic Engineering* (Rotterdam)

[2] Landbø T 2013 *OO Star Wind Floater A robust and flexible concept for floating wind*

[3] Luan C, Michailides C, Gao Z and Moan T 2014 *Proc. of the ASME 2014 33rd Int. Conf. on Ocean, Offshore and Arctic Engineering* (California)

[4] Ishihara T 2013 *Fukushima Offshore Wind Consortium* (Fukushima FORWARD)

[5] Bachynski E E, Chabaud V and Sauder T 2015 *12th Deep Sea Offshore Wind RD Conference* (Trondheim)

[6] Michailides C, Luan C, Gao Z and Moan T 2014 *Proc. of the ASME 2014 33rd Int. Conf. on Ocean, Offshore and Arctic Engineering* (California)

[7] Jonkman J M, Butterfield S, Musial W and Scott G 2009 *NREL report*

[8] Jonkam J M 2010 *NREL report*

[9] Faltinsen O M 1990 *Sea loads on ships and offshore structures* (Cambridge University Press)

[10] Hansen M O L 2008 *Aerodynamics of wind turbines* (London: Earthscan)

[11] Jonkman J M and Kilcher L 2012 *Turbsim Users' Guide*

[12] IEC 2005 *IEC 61400-1. Wind Turbine - Part 1 : Design requirements.*

[13] Zhao R and Faltinsen O M 1988 *J. Applied Ocean Research* **10** 87-99

[14] Chakrabarti S 1984 *J. Applied Ocean Research* **6** 73-82

[15] DNVGL 2013 *DNV-OS-E301,Position Mooring*

[16] DNVGL 2011 *DNV-RP-C205,Environmental Conditions and Environmental Loads*

[17] Li L, Gao Z and Moan T 2015 *J. of Offshore Mechanics and Arctic Engineering* **137** 031901-1-16

[18] Naess A and Moan T 2013 *Stochastic dynamic of marine structures* (Cambridge University Press)

[19] Gao Z and Moan T 2007 *J. of Applied Ocean Research* **29** 45-54

[20] Gao Z and Moan T 2009 *Proc. of the 10th Int. Conference on Structural Safety and Reliability* 997-1004

[21] Li H , Du J, Wang S, Sun M and Chang A 2016 *J. of Ocean Engineering* **124** 204-214

[22] Stansberg C T 2008 *Proc. of the ASME 27th Int. Conf. on Offshore Mechanics and Arctic Engineering* (Estoril)